Critical-Density Scale-Length Measurements in Laser-Produced Plasmas

Steven Jackel, James Albritton, and Edward Goldman
Laboratory for Laser Energetics, College of Engineering and Applied Sciences, University of Rochester, Rochester, New York 14627
(Received 2 June 1975)

Inhomogeneity scale lengths between critical and quarter-critical densities have been obtained by photographing laser-produced plasmas in emitted light at twice and three-halves the laser frequency. The displacements of the harmonic-light images were measured on photographs taken from a position below spherical targets irradiated by four Nd:glass-laser beams. Over the range of 5 to 20 J absorbed (in 200 to 600 psec) by 70–100-μm-diam glass shells, this scale length increased linearly from 10 to 30 μm.

In laser-induced-fusion schemes,[1] the fuel-pellet plasma near the radiation-propagation cutoff density must exhibit strong coupling to the heating pulse. The dominant contribution to classical absorption of the light[2] occurs where the laser frequency is near the plasma frequency, and most collisionless mechanisms responsible for anomalous absorption and reflection[3,4] are enhanced there. Indeed the radiation-plasma interaction is sensitive to the inhomogeneity scale length of the critical-density plasma.[2-4] Characterization of this region in high-energy experiments is therefore important to the understanding of laser-plasma physics.

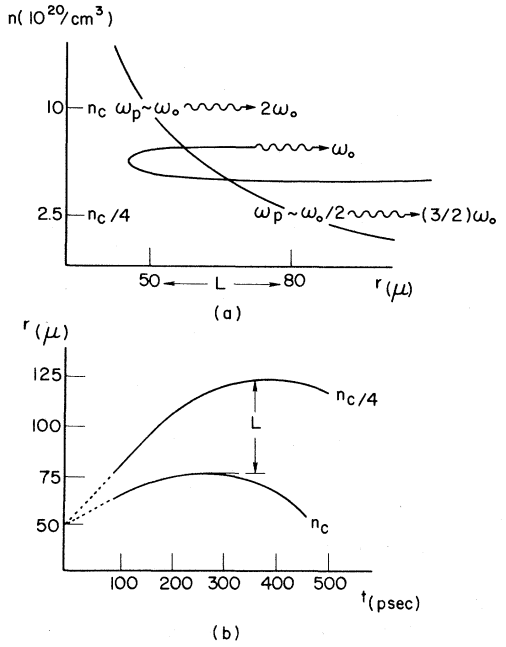

FIG. 1. (a) Target density profile and harmonic-emission regions at a fixed time. (b) Trajectories of critical and quarter-critical densities during the heating pulse.

Here we report critical-density scale-length measurements obtained by photographing laser-produced plasmas in second- and three-halves-harmonic emitted radiation. Figure 1 shows a typical target density profile and the trajectories of the emitting critical and quarter-critical phase points during the laser pulse from a hydrodynamic simulation of our experiments.[5] Note that the pulse spans the entire time of expansion of the two phase points.

The literature[6,7] strongly suggests that the origin of the second-harmonic light is the critical-density plasma, $n_c \simeq 10^{21}/\mathrm{cm}^3$ for $\omega_0 \simeq 2\times 10^{15}/\mathrm{sec}$. Nonlinear beat currents between electron plasma waves at $\omega_p \simeq \omega_0$ and the laser at ω_0 can be expected to emit $2\omega_0$ radiation from the inhomogeneous plasma. Similarly the $\frac{3}{2}\omega_0$ light is likely to eminate from quarter-critical density,[8,9] $n = n_c/4 \simeq 2.5\times 10^{20}\ \mathrm{cm}^{-3}$, as a result of beating between the laser and plasma waves at $\omega_p = \omega_0/2$. Since

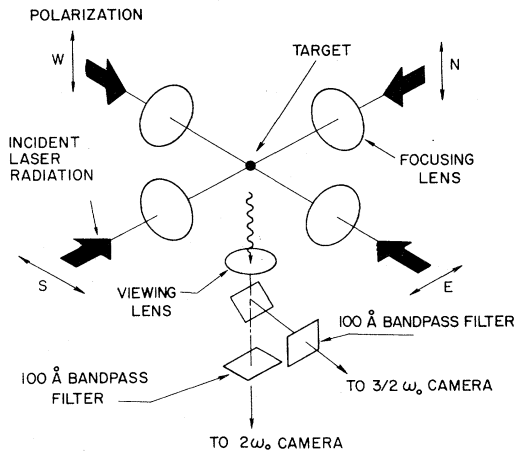

FIG. 2. The experimental facility with four coplanar beams. Harmonic-light photographs are taken from below the target.

the harmonic signals are launched at densities well below their cutoff, $4n_c$ for $2\omega_0$ and $\frac{9}{4}n_c$ for $\frac{3}{2}\omega_0$, they should leave the plasma along nearly straight rays. In this model, the critical and quarter-critical densities can be clearly distinguished by their harmonic-light signatures.

Time-integrated photographs were taken perpendicular to the plane of illumination of spherical-glass-shell targets. The four-beam Nd:glass-laser system[10] is illustrated schematically in Fig. 2 and a pair of the harmonic-light photographs is reproduced in Fig. 3(a). For the sake of definitiveness we call the distance between the critical and quarter-critical densities, both calculated and observed, the plasma inhomgeneity scale length. A more rigorous description of the profile involves details to which our methods are presently insensitive. The distances were measured between the outer edges of the harmonic images. This scale length was found to increase linearly with absorbed energy over the range investigated. Parallel to this work we have begun to develop a shot-by-shot diagnostic of target illumination quality and a visualization of the parametric-wave interaction zone. Similar efforts have been reported recently on single-beam, slab-target experiments.[11]

The targets were illuminated by use of 20-cm-focal-length $f/2$ aspheric lenses which focused 85% of the beam energy in spots of 85 μm diameter and 85 μm axial extent. The photographic apparatus employs a viewing lens a few degrees off the perpendicular axis below the target. Chromatically corrected optical elements were used to transport and focus the $2\omega_0$ and $\frac{3}{2}\omega_0$ light emitted by target onto Kodak Tri-X and High-Speed-Infrared films, respectively. The spatial resolution through the system in white light is less than 10 μm and the depth of field is 200 μm.

The series of experiments considered in this paper were performed with glass shells 70 to 110 μm in diameter with wall thicknesses of 1 to 2 μm. The structural quality of the targets (sphericity and concentricity) is not relevant to the results presented here. Heating-pulse parameters for *each* of the four beams ranged in energy over 5 to 40 J in 200 to 600 psec. The smallest targets did not completely occlude the beams but were still subjected to intensities of greater than 10^{15} W/cm^2. The energy absorbed by the plasma was measured as the sum of the energy in charged particles (Faraday-cup collectors) and in x rays (silicon p-i-n detectors).[10] Absorbed energies ranged from 10 to 30% of the incident energies

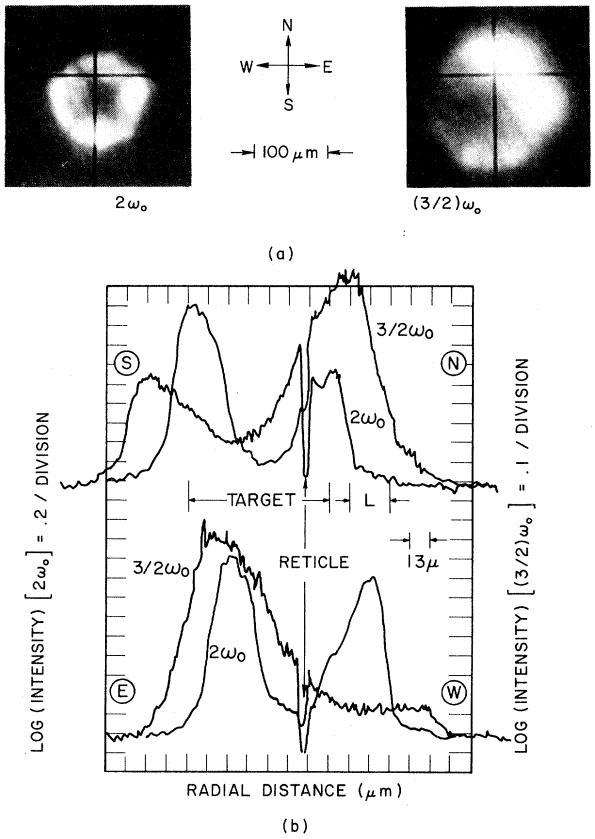

FIG. 3. Shot number 9912: 58 J incident in 550 psec, 18 J absorbed by 92-μm×1.3-μm glass shell. (a) Harmonic-radiation photographs of the target. (b) Microdensitometer traces of photographs in (a).

with the larger targets and longer pulses giving the higher figures.

Microdensitometer traces across the photographs, Fig. 3(b), quantify the displacement of the emission regions of the harmonic light in the plasma. Figure 4 shows that the significant features of the traces can be obtained by modeling the emitting regions as optically thin shells moving with the density phase points. For a homogeneous distribution of sources within the shell, the intensity of emission is proportional to the projected shell thicknesses along the direction of observation. Refraction of the incident light by the plasma is important in defining the lateral extent of the interaction-emission zones. Refraction of the emitted light does not affect the intensity profiles except to broaden the inner shoulders of the traces.

Important features of the model with regard to interpretation of the data are the localization of the image and its sharp outer boundary which

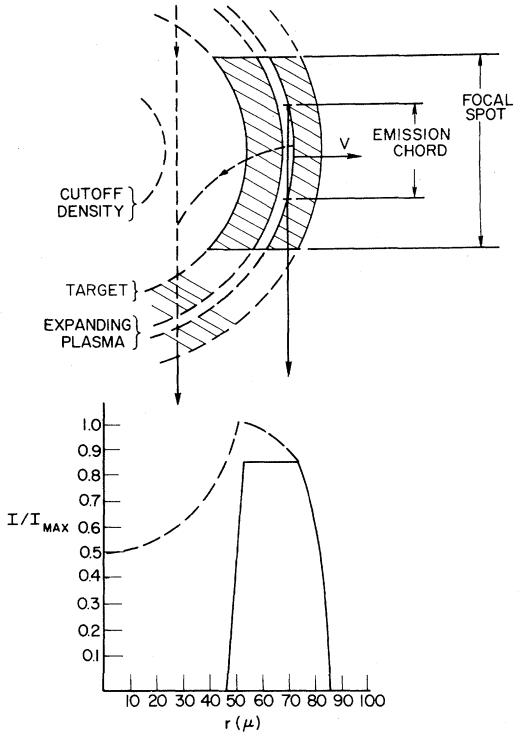

FIG. 4. An optically thin isotropically radiating shell and its image intensity profile through the photographing system.

corresponds closely to the maximum excursion of the radiating shell. In general, the computed traces were insensitive to the details of the time history of the density profile predicted by computer codes. Thin dynamic shells would, however, appear much like thick stationary shells in the traces.

Photos at $2\omega_0$ taken through one of the illuminating lenses confirmed that the active region is indeed smaller than most of the targets and much like the free-space focal-spot size. The $\frac{3}{2}\omega_0$ traces in Fig. 3(b) indicate that a complete shell is emitting. Note that any light transmitted by the 100-Å-bandpass filters other than the $2\omega_0$ and $\frac{3}{2}\omega_0$ harmonics must be of considerably less intensity. This can be deduced from the extremely low levels of light observed outside of the rings where the theories of harmonic-light production predict none.

For the shot illustrated in Fig. 3, an inhomogeneity scale length of 26 μm is measured between the outer edges of the two densitometer traces. A hydrodynamic velocity of the order of 5×10^6 cm/sec is estimated by dividing the scale length by the pulse length. The measured scale

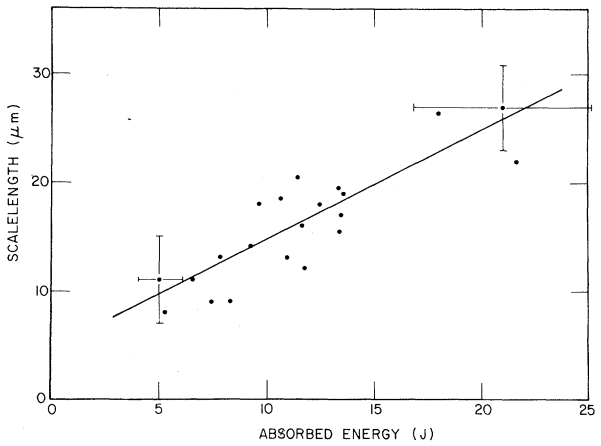

FIG. 5. Averaged north-south and east-west inhomogeneity scale length between (2.5 and 10) $\times10^{20}$/cm^3 plotted versus absorbed energy.

length and estimated velocity are in fair agreement with the computer simulation of the experiment.

The complete data are presented in Fig. 5 where the plotted scale lengths are an average of north-south and east-west measurements. Over the range of 5- to 20-J absorbed energy the scale length increases linearly from 10 to 30 μm. The classical absorption fractions[2] estimated by use of the measured scale lengths agree pointwise with those observed experimentally. The absorption fraction also increases with absorbed energy.

[1]J. Nuckolls, J. Emmett, and L. Wood, Nature (London) 239, 139 (1972).

[2]J. Dawson, P. Kaw, and B. Green, Phys. Fluids 12, 875 (1969).

[3]N. G. Denisov, Zh. Eksp. Teor. Fiz. 31, 609 (1956) [Sov. Phys. JETP 4, 544 (1957)].

[4]A. A. Galeev, G. Laval, T. O'Neil, M. N. Rosenbluth, and R. Z. Sagdeev, Zh. Eksp. Teor. Fiz. 65, 973 (1973) [Sov. Phys. JETP 38, 482 (1974)].

[5]E. Goldman, Laboratory for Laser Energetics, University of Rochester, Report No. 16, 1973 (unpublished).

[6]N. S. Erokhin, V. E. Zakharov, and S. S. Moiseev, Zh. Eksp. Teor. Fiz. 56, 179 (1969) [Sov. Phys. JETP 29, 101 (1969)].

[7]K. Eidmann and R. Sigel, Phys. Rev. Lett. 34, 799 (1975).

[8]D. Biskamp and H. Welter, Phys. Rev. Lett. 34, 312 (1975).

[9]P. Koch and J. Albritton, Phys. Rev. Lett. 34, 1616 (1975).

[10]M. Lubin, E. Goldman, J. Soures, L. Goldman, W. Friedman, S. Letzring, J. Albritton, P. Koch, and

B. Yaakobi, in *Proceedings of the Fifth International Conference on Plasma Physics and Controlled Nuclear Fusion Research, Tokyo, Japan, 1974* (International Atomic Energy Agency, Vienna, Austria, 1975).

[11]A. Saleres, M. Decroisette, and C. Paton, Opt. Commun. 13, 321 (1975).

Warm-Plasma Effects on Fast-Alfvén-Wave Cavity Resonances

D. G. Swanson and Y. C. Ngan
Department of Electrical Engineering, University of Southern California, Los Angeles, California 90007
(Received 10 February 1975)

Whereas experiments on the ST Tokamak demonstrated fast-Alfvén-wave cavity resonances to be sharp and resolvable and suggested highly efficient coupling could be obtained for plasma heating, warm-plasma effects appropriate to fusion plasmas suggest such resonances will not be resolvable and that the characteristic mode structure will be significantly modified through the coupling to ion-Bernstein modes unless the heating is shifted to higher harmonics of the ion-cyclotron frequency.

Experiments on the ST Tokamak employing the fast Alfvên wave for plasma heating at the first harmonic of the ion-cyclotron frequency ($\omega = 2\Omega_i$) demonstrated sharp peaks in the antenna-loading impedance whenever the wave frequency matched a cavity-resonance frequency of the toroidal cavity.[1] The high potential efficiency of such cavity-resonance rf heating makes the scheme attractive for fusion-plasma heating. As experiments progress toward fusion parameters, however, the resonance widths will become broader and the mode spacing smaller so the modes may overlap. We also find mode conversion and tunneling effects due to coupling with ion-Bernstein modes which may completely change the mode structure. These effects are investigated for the first few harmonics of the ion-cyclotron frequency.

Whereas toroidal effects in a cold plasma have been shown to be important in the propagation of the ion-cyclotron wave,[2-5] they have at the same time been shown to be relatively unimportant in the propagation of the fast Alfvén wave except for a slight cavity-resonance shift to lower frequency. The damping is also affected by toroidal effects since only a small fraction of the cross section of the torus is resonant at the fundamental or harmonic of the ion-cyclotron frequency. Therefore, except for the damping modification, we shall neglect the toroidal effects and concentrate on temperature effects through finite-Larmor-orbit corrections in order to calculate the cavity-resonance widths. Perkins *et al.*[5] have estimated the damping decrement for the fundamental and first harmonic, the latter of which has the same form as our result but differs by a factor of about 3.

Employing for the most part our previous notation and formalism[6] for the warm plasma in a cylindrical wave guide, we restrict our problem to that of determining the wave-guide cutoff, defined by $k_\parallel = 0$ (or no azimuthal variation about the major axis in a torus). In this case, the plasma solutions decouple into transverse-electric and transverse-magnetic modes so that the fast-Alfvén-wave cutoff condition becomes

$$k_\perp^2 K_1' = K_1'(K_1' + 2K_0') + K_2'^2, \tag{1}$$

where for $T_{\perp i} = T_{\parallel i}$, with no drift velocity and cold electrons ($\lambda_e = 0$, $|\omega \pm n\Omega_e| / k_\parallel V_e \gg 1$),

$$\begin{aligned}
K_1' &= \frac{\omega^2}{C^2}\left[1 + \frac{\omega_{pi}^2 \exp(-\lambda_i)}{\omega k_\parallel V_i} \sum_{n=-\infty}^{\infty} \frac{n^2 I_n(\lambda_i)}{\lambda_i} Z\left(\frac{\omega + n\Omega_i}{k_\parallel V_i}\right)\right], \\
K_2' &= \frac{i\omega\omega_{pi}^2 \exp(-\lambda_i)}{C^2 k_\parallel V_i} \sum_{n=-\infty}^{\infty} n[I_n(\lambda_i) - I_n'(\lambda_i)] Z\left(\frac{\omega + n\Omega_i}{k_\parallel V_i}\right) - \frac{i\omega\omega_{pi}^2}{C^2\Omega_i}, \\
K_0' &= \frac{\omega\omega_{pi}^2 \exp(-\lambda_i)}{C^2 k_\parallel V_i} \sum_{n=-\infty}^{\infty} \lambda_i[I_n(\lambda_i) - I_n'(\lambda_i)] Z\left(\frac{\omega + n\Omega_i}{k_\parallel V_i}\right),
\end{aligned} \tag{2}$$

where $\lambda_i = k_\perp^2 V_i^2 / 2\Omega_i^2$ and we have not yet let $k_\parallel \to 0$. In an actual heating experiment, there will be at

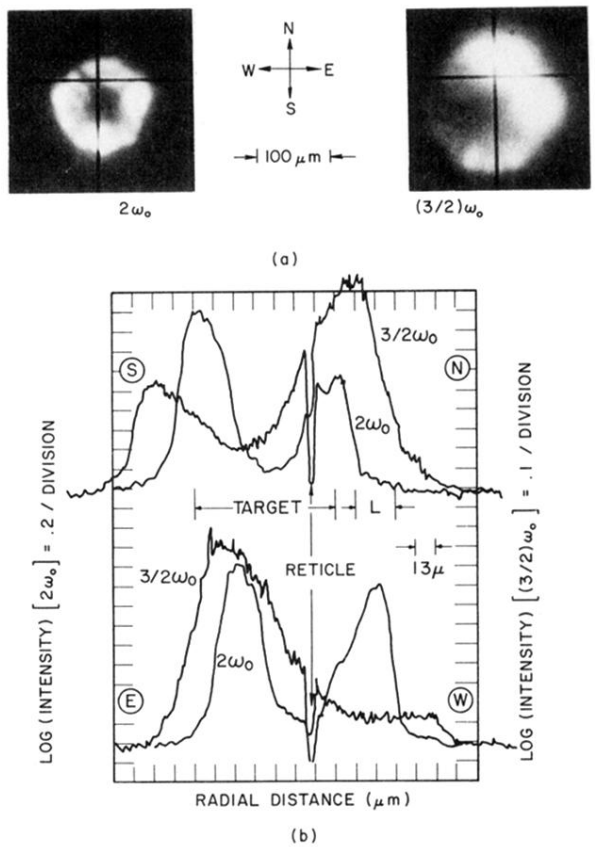

FIG. 3. Shot number 9912: 58 J incident in 550 psec, 18 J absorbed by 92-μm$\times$1.3-μm glass shell. (a) Harmonic-radiation photographs of the target. (b) Microdensitometer traces of photographs in (a).